Replication and Experimental Characterization of the Wallace Dynamic Force Field Generator

C. Boy[1], I. Lőrincz[2] and M.Tajmar[3]

Institute of Aerospace Engineering, Technische Universität Dresden, 01062 Dresden, Germany

In the 1970s, Henry W. Wallace filed a number of patents claiming that the rotation of masses with a net nuclear spin leads to the generation of a gravity-like force field that effects other rotating masses as well as heat conductivity. Based on his patent drawings we designed an experimental apparatus as close as possible to his original design including features to mount precision laser sensors to record speed and orientation of the rotating masses. It consists of a generator and a detector assembly with rotating masses as well as a massive top and bottom part of the same spin-polarizable material in order to provide an effective pathway for the claimed field. We chose brass with about 60% of Copper that is spin-polarizable. The assembly weights around 150 kg. Both assemblies can be rotated using compressed air up to 28,000 RPM as in the Wallace patents. Wallace claimed that the oscillation period of the rotating detector mass, oscillating around a knife-edge support along its middle-axis, varies with the orientation of the generator assembly. This could be explained by either magnetic or indeed anomalously large frame-dragging fields. Therefore, in addition to the detector assembly, we implemented magnetic field sensors, accelerometers as well as a high-performance laser-gyroscope in order to investigate possible magnetic influence and direct gravitational and frame-dragging signals. Here we report on the construction as well the results of our measurement campaign with, up to our knowledge, the first replication of the Wallace dynamic force field generator. We did find an anomaly in the oscillation of the detector gyroscope similar to the claim of Wallace, but we could trace it back to a vibration artefact.

Nomenclature

A	=	area
a	=	acceleration
c_w	=	drag coefficient
F_w	=	drag force
F_R	=	restoring force
g	=	gravitational acceleration = 9.8065 m s^{-2}
h	=	height
J	=	torque moment
J_0	=	torque moment (with respect to rotation axis outside of center of mass)
m	=	mass
r	=	distance
s_r	=	distance of displacement (amplitude)
T	=	oscillation period
v	=	velocity
x, y, z	=	Cartesian coordinate (linearly independent)
α	=	angle
ρ	=	density
ω	=	angular frequency

---

[1]PhD student, Space System Chair, christian.boy@tu-dresden.de
[2]PhD student, Space System Chair, istvan.lorincz@tu-dresden.de
[3]Professor, Institute Director and Head of Space Systems Chair, martin.tajmar@tu-dresden.de, Senior Member AIAA.

I. Introduction

Overcoming the gravity field of the earth is one of the most fascinating quests of science and engineering. Advantages could be made in terrestrial applications as well as in the energy management for space applications. Manipulating the weight of bodies could be a very useful possibility to make all known propulsion techniques more effective. Creating a force field that operates toward the gravity field of the earth could for example decrease the needed propellant for rocket launches. This would allow an increase in the payload mass with the same system mass. It could also be possible to generate artificial gravity on space stations or modify orbit maneuvering and flight paths of satellites.

The American engineer Henry W. Wallace patented three practical experiments in the early 1970s claiming to have generated a secondary gravitational field using high-speed rotation of highly spin-polarizable mass[1-3]. In his later patents, he also designed a gravity field generator[2] as well as a heat pump[3] based on this principle. He built a structure with relatively moving bodies working in a closed loop of the same material that shall create a secondary gravitational field caused by the spin polarization of the unpaired nucleons. Comparable to the Barnett-Effect[4], where the macroscopic angular momentum of a rotating iron rod is transferred to the microscopic spin of the electrons to polarize them, he claimed that the rotation of a brass wheel could be transferred to the spin of the nucleons. Caused by its polarization and the resulting superposition, these atomic nuclei develop a measurable so-called kinemassic field that works against or toward the gravitational field depending on their moving direction. He claimed that this field is non-electromagnetic in nature and exhibits frame-dragging-like characteristics similar to what we expect from general relativity[5,6] but many orders of magnitude higher.

For the first time, we manufactured an optimized reproduction of the Wallace invention to verify his claims and to investigate the measured effects.

II. Historical Set-up by Henry W. Wallace

The original patents of Henry Wallace contain a detailed explanation of his experimental set-up and its operating principles. He explains his construction and its functionality with all important facts based on his conclusion to polarize the atomic nuclei spin of a material to create a force field using high-speed rotation. The complete set-up is divided in two main assemblies – one to create the force field circuit and the other to mount the parts of the primary circuit assembly.

A. Construction and functionality

The complete structure is shown in **Fig. 1** on the left side. The mentioned assembly with the parts to mount the circuit members (1) is grey colored and have the function to calibrate and hold the field creating parts and assemblies. The adjustment of the generator and detector assemblies was realized with clamping claws which were fixed at the ground plate. The generator (3) produces the force field that will be transferred over the upper and lower mass member (2) to the knife edge mounted and oscillating detector (4) that closes the field circuit. Important to mention are the air gaps between the mass members and the generator and detector. These distances influence the transferred effect and further the generated field strength. Another possibility to influence the resulting field strength is to change the effective direction of the generated force field by turning the generator on its mounting axis. It is mounted on the base structure about two ball bearings that made it possible to change the angle of the vector field.

On the right side of **Fig. 1** the partial section of the generator with its most important parts is shown. The frames (1) act as the basic structure as all parts are mounted on it. Two pole halves (2) are connected to the poles with screws (8) and are adjustably fixed on the frame with setting screws (7) to compose the upper and lower poles. The ball-bearings (5) are mounted in the center of the frame and bear the wheel (3). It rotates while maintaining a small distance to the pole planes with a speed up to 28,000 rpm and is powered with compressed air by a nozzle (4).
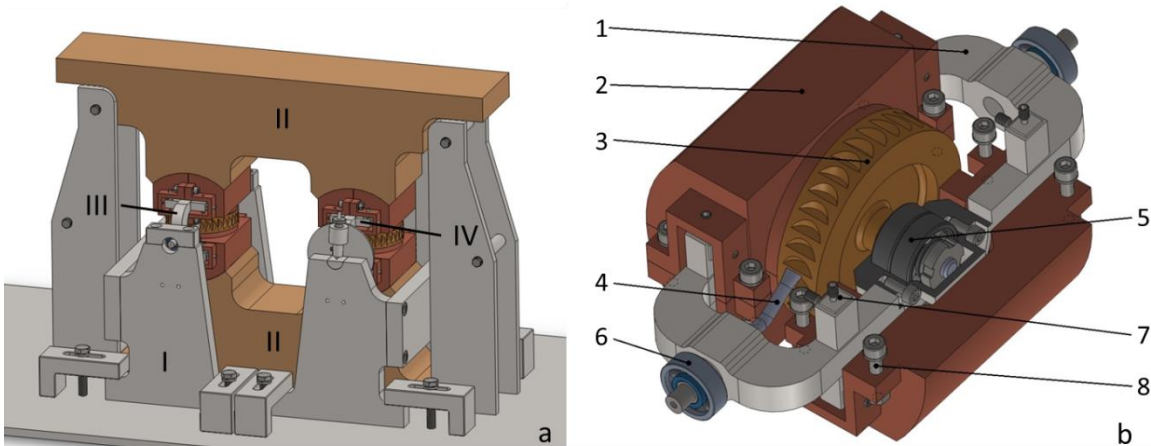
a) CAD model of the complete original set-up according to Wallace[1,2]

b) The field creating generator in detail.

Figure 1   Original Design of the Wallace Experiment.

An important aspect is the choice of the used material for the assemblies. The field creating parts of the circuit are made of a special brass alloy with a high percentage of copper that is the polarizable ingredient of the used material. The number of positively charged protons defines the element while the number of neutrons defines the isotope of the element. The sum of both sets the mass number that further gives information about the capability of a nuclear spin. If the isotope has an odd mass number it owns a spin, otherwise not. Stable elements on Earth mostly include more than one isotope but not all of them have a net spin. So the percentage of isotopes with a spin has to be very high to generate the forecast effect. For example the element nickel consists of five stable isotopes but only one of them (^{61}Ni) owns a spin of just 1.14% of relative occurrence. Copper in contrast has two stable isotopes (^{63}Cu and ^{65}Cu) and both have useable spins.

B. Measurement results

The main experiment and its following measurement diagram were explained in his first publication. While both flywheels were energized and turned with a speed of more than 20,000 rpm, the effective direction of the generator was changed with respect to the detector. The direction changed from clockwise to counterclockwise with respect to the coordinate system of the set-up over a period of 65 minutes. To measure the amplitude Wallace used a mirror which was fixed at the detector and reflecting the beam of a light source to a calibrated wall screen. The detector, mounted on knife-edges and oscillating with a time period of 11 seconds and an average amplitude of 130 arc minutes (=2.1 degrees), exhibited a rising amplitude after changing the effective direction of the generator. The measurement result, published by Wallace and shown in **Fig. 2**, reveals the created effect in the rising amplitude of 25.5 arc min (=0.4 degrees) after changing the effective direction of the generator.
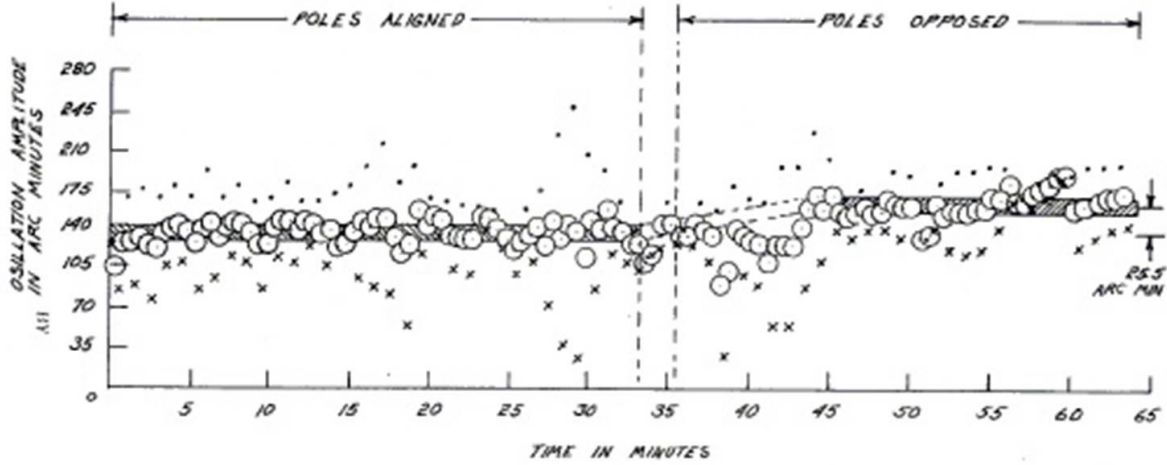
Figure 2   Variation of the Detector Oscillation as measured by Wallace[1].

This effect gives information about the existence of a possible force field that's working toward the gravity field. According to the mode of operation of a physical pendulum, his experiment can be explained by the formula for an oscillating mass with

$$T = 2\pi k \sqrt{\frac{1}{g}}, \text{ with } k = \sqrt{\frac{J}{mr}}.$$

(1)

Therefore the existence of a secondary force field that acts against or toward gravitational acceleration adds up to

$$T = 2\pi k \sqrt{\frac{1}{(g \pm a)}}, \text{ (a} \leq \text{g)},$$

(2)

and it is obvious that the time period of the oscillation will increase with a reduced value for acceleration. The direct correlation to the amplitude (s_r) is given by the simultaneously changing of the restoring force (F_R) with

$$s_R = -r\frac{F_R}{m(g \pm a)}.$$

(3)

## III.   Constructive optimization

Reducing the costs for material and manufacturing, improving handling of the complete structure and increasing the reliability were the main subjects for optimization of the reproduction. Based on the technical specifications (e.g. air gaps, used alloys, rotation speed, etc.) of the patents it is necessary to make a few modifications to guarantee safe and reliable performance.

A. Redesign of the Set-up

The first step to reconstruct the experimental set-up was to simplify the parts and assemblies that have no active function to the mode of operation. The basic structure was modified to an assembly with commercial off-the-shelve (COTS) profiles that just needed to be fixed by screws. The dimensions of the three mounting planes for the lower mass member (ground plate - I), the generator and detector (main beams - II) and the upper mass member (cross beams - III) were determined, which in turn defined the distances between the circuit parts (shown in **Fig. 3a**). The planes perpendicular to the ground plane define the position for the generator (IV) and the detector and measurement systems (V) and are adjustable about specially assemblies.
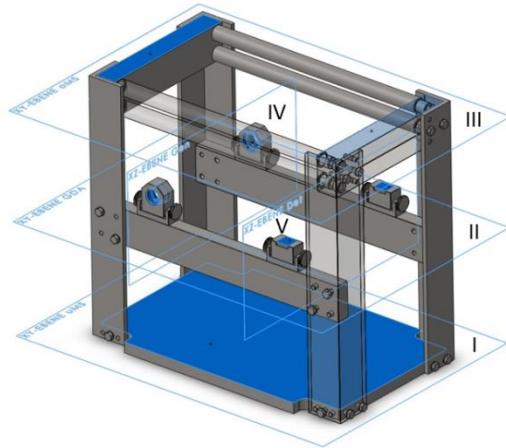
a.) Redesigned basic structure with mounting planes for the circuit parts
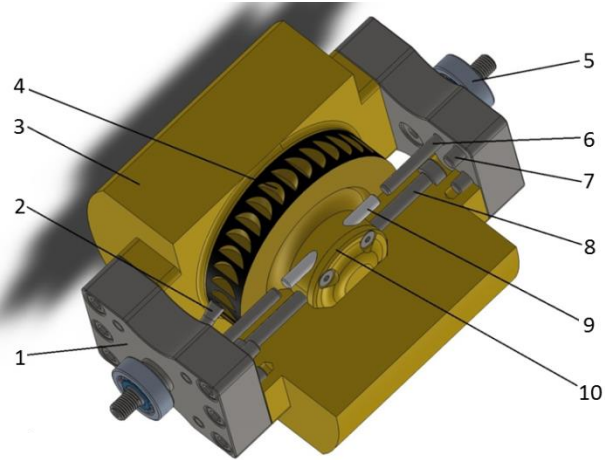
b.) Redesigned field creating generator in detail

Figure 3   Redesigned Setup.

The most important modification received the generator (shown in **Fig. 3b**). The frame was replaced by flanges (1) that were fixed by screws (7) and parallel pins (6). Thereby it was possible to use complete poles (3) and to integrate the bearing cases (10) for the wheel bearings which are also fixed by screws (8) and parallel pins (9). The fly wheel was centered with a steel shaft while the air gaps between the pole planes were adjustable with shim rings. The basic geometry of the mass members was unchanged but their length was reduced to the overall length of the complete structure.

B. Design and FEM analysis of used material for the flywheel

One of the requirements was the high rotation speed of the field generating flywheel. Rotation speeds up to 28,000 rpm induce very high centrifugal forces and further a very strong material strain. The used alloy with a high percentage of copper (89% Cu, 10% Zn, 1% Pb) has a low tensile strength and an unbalance could be very dangerous.

The sectional view and the strain analysis result of the original wheel (material and design) are shown in the upper section of **Fig. 4**. In comparison to an ideal flywheel design with a form factor of 1.0 Wallace's design only results in a form factor of 0.4. This leads to an uneven load distribution along the flywheel's cross section as it is depicted in the figure. The red area next to the rotation axis indicates a high tensile strain and the imaged scale shows that it could lie beyond the maximum of the acceptable range. A rule of thumb is to set the minimum safety factor to 2 for the dynamic strain. This is just possible by changing the used material and optimizing the geometry to distribute the load nearly uniform over the whole radius.

The bottom picture in **Fig. 4** shows the resulting new design of the flywheel after analysis using another brass alloy with less copper (59% Cu, 28% Zn, 3% Pb) but the possibility to increase the maximum speed up to 48,000rpm (the rotation speed limit of

Figure 4   Design and strain analysis of the flywheel by Wallace (top) and redesigned flywheel with strain analysis (bottom).

the ball bearings). The scale on the right shows that the load on the redesigned wheel was reduced an order of magnitude, compared to the original. Alternatively an alloy with 98% Copper and 2% Beryllium could be applied[7]
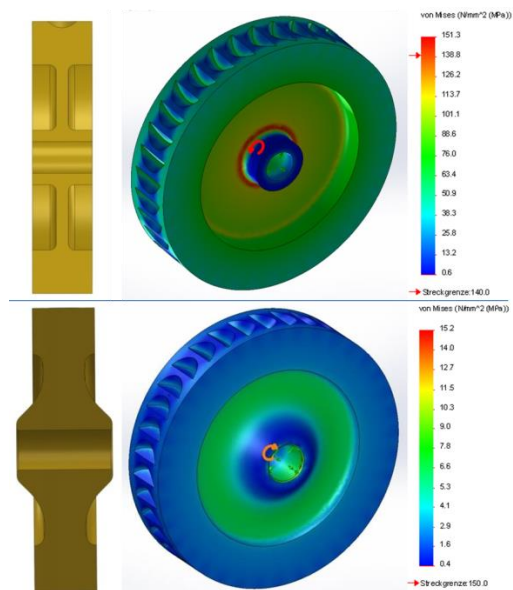
but it is more expensive and more complicate to manufacture (e.g. it is harmful to health to grind his alloy without cooling).

C. Chosen materials for circuit and mounting assembly

Despite the claimed point that the generated field is non-electromagnetic in nature the polarization of nuclei spin is always connected with the polarization of the magnetic moment of the nuclei. This could further mean a possible magnetization of the surrounded parts and assemblies using a conventional structural steel (S235JR) like the original set-up. To minimize this potential risk the chosen material for the structure parts is a stainless steel alloy (X5CrNi18-10) which has a significantly lower magnetizability. This alloy also includes less polarizable isotopes than the structural steel which further decouples the circuit parts from each other. With the elements included and their isotopes this alloy has a total polarizability of 2.54 percent. Referring to the mentioned material conditions for the flywheel the replaced material for all circuit parts and assemblies were made of the same alloy. It can be well manufactured and includes an adequate ratio of polarizable isotopes. The complete redesigned, manufactured and installed experimental set-up is shown in **Fig. 5**.
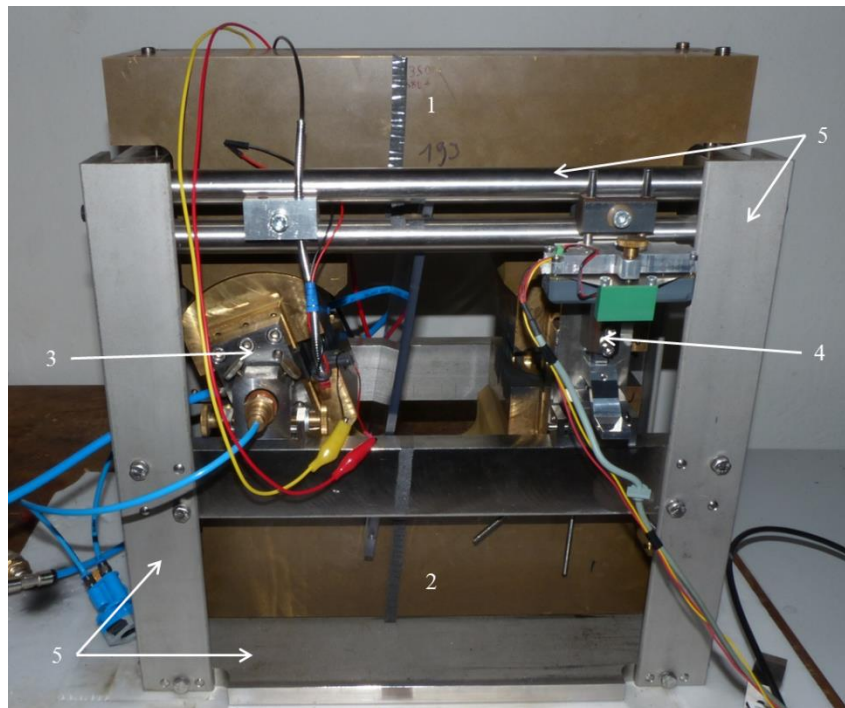

Figure 5   Complete redesigned and installed set-up with its main parts: Upper (1) and lower (2) mass member, Generator (3), Detector (4) and the structural components (5)

IV.   Measurement systems and methods

One property of the generated force field predicted by Wallace is its non-electromagnetic nature. Hall-sensors were used to prove this assumption with an adequately method. An accelerometer is used to evaluate the existence of a secondary force field. The Hall-sensors and accelerometers were combined in one system to measure all three axes independently. We characterized the sensors over a longer time to estimate their thermal drift as well as performed reference measurements with them in order to do a proper calibration. In addition, we implemented a laser gyroscope that can directly measure any frame-dragging effect as claimed by Wallace. Referring to Wallace's published measurement results, the impact from the induced field should be easily detectable by a gyroscope as it should be orders of magnitude higher than the one induced by the earth's rotation. For these measurements, we removed the detector assembly and positioned our measurements box in its place with spin-polarizable covers on the top and bottom in order to channel the generated fields optimally through our sensors as shown in **Fig. 6**.

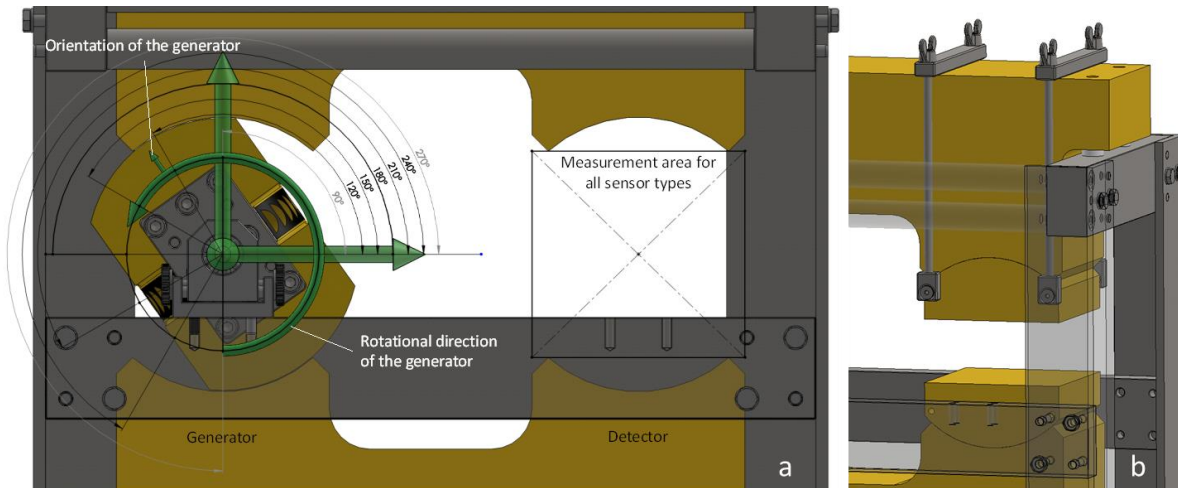American Institute of Aeronautics and Astronautics

Figure 6   Measurement strategy and detection area for all sensors (a) and additional manufactured components to limit the measurement space for the sensor boxes (b).

The last measurement system was the original one from Wallace's publication. A detector (identical in construction with the generator) was mounted with knife edges on hardened steel plates and is able to oscillate nearly frictionless. The distance between its balance point and the mounting point was designed to be adjustable in order to set the claimed oscillation period. The claimed effect should manifest in a changing the oscillation period and an increased amplitude.

A. Hall-sensor and accelerometer

The utilized magnetic sensors (Honeywell SS 495) have a measurement range of ±0.115T. As gyroscopes and accelerometers are influenced by magnetic fields, this measurement was important for our later frame-dragging assessment. **Fig. 7** shows the results of the signals measured in the principal direction with aligned poles in the middle diagram and opposed poles in the bottom diagram depending on the rotation speed pictured in the top diagram. Only the thermal drift rate and the noise level of the sensors are visible after turning-off the compressed air. The measured noise of +/- 2.10^{-4} T is within the range of the reference measurement and the drift rates corresponding to the characteristic of the sensors specifications. These magnetic fields can not influence our gyroscopes and accelerometers within their resolution. The coupling factor between the linear fit and the falling rotation speed is five times lower than the standard deviation for the sensors and shows that there is no speed-dependent variation of the measurement results.

The used accelerometers (Colibrys SF1600S) have a measurement range of ±3g with a maximum noise level of $0.3\mu g_{rms}/HZ^{1/2}$ and a thermal drift rate of $1.2\times10^{-4}g/°C$. This resolution allows the detection of the predicted effect with a significantly higher precision than required. **Fig. 8** shows the diagrams with the measurement results of the accelerometers also depending on the rotation speed (top diagram). It is quite clear that the accelerometers show a big noise while the generator wheel is spinning up due to the loud acoustic noise of the compressed air as well as from secondary air streams towards our measurement box. After stopping the airflow on the flywheel, the measured acceleration in both directions was nearly constant and at a value of 1g with a deviation smaller than the noise level. So also here, the accelerometers show no rotation-speed dependent reaction after comparing the linear fit and the falling rotation speed. The small variations at 100Hz and 300Hz are vibrations that were transferred from the set-up table over the ground to the measurement table where the sensors were fixed.
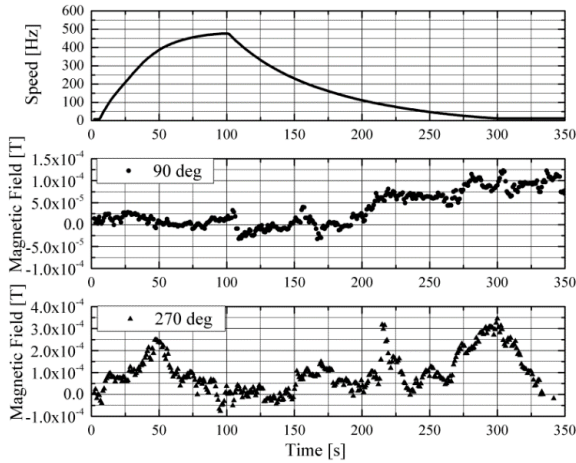
Figure 7 Diagrams of the generator wheel angular velocity (top) and the associated measured data of the Hall sensors for the aligned (middle) and opposed (bottom) orientation of the rotating generator
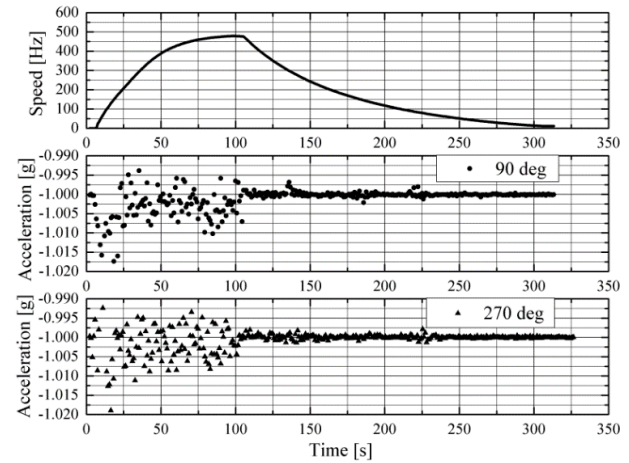

Figure 8 Diagrams of the generator wheel angular velocity (top) and the associated measured data of the accelerometers for the aligned (middle) and opposed (bottom) orientation of the generator.

B. Gyroscope

Detecting his predicted frame-dragging like effect a very precise optical gyroscope was used. This instrument (KVH-DSP 3000) is able to measure a maximum angular velocity of $\pm375°/s$ with a resolution of $0.005°/s$ (8.727×10^{-5} rad/s). The thermal drift rate amounts to $6°/hr$ during a change in temperature less than 1 K/min and its noise level is $4°/hr/Hz^{1/2}$ (6.98×10^{-3} rad/hr/Hz$^{1/2}$). The pictured diagrams in **Fig. 9** show the measurement results of the gyroscope during the aligned and opposed effective orientations of the generator. They are plotted directly against the flywheel's rotation speed allowing a clear determination that there was no measurable effect outside the noise level.
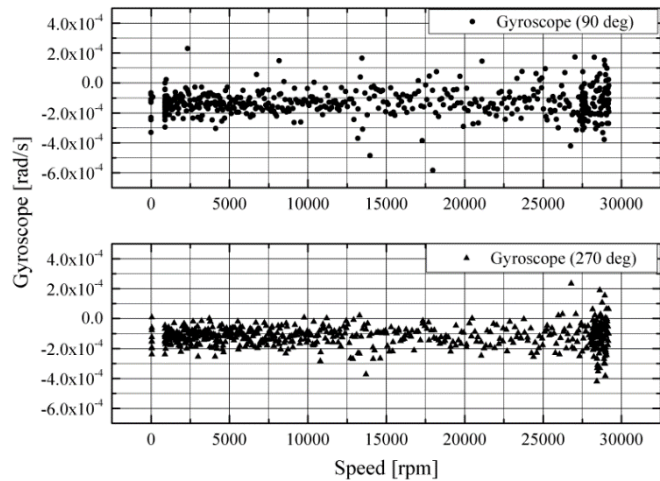
C. Oscillator

Figure 9 Gyroscope signals depending on flywheel speed to aligned (top) and opposed (bottom) direction.

The last and most important measurement is the experiment based on the original one from the patent. A detector assembly constructed in the same way like the generator but mounted on knife edges was oscillating during which the generator wheel was accelerated up to 30,000 rpm. Wallace write that his detector wheel was rotating. However, it is clear that the rotating detector wheel will significantly change the oscillation period and amplitude without any action of the generator if it is also rotating at high speeds due to precession forces. We tried this configuration and observed that indeed the spinning detector will try to perfectly align its spinning axis and therefore no oscillations can be seen. Therefore, all results were measured with the detector flywheel not spinning and just the variation in oscillation periods and the amplitudes were measured. An experiment with the technical conditions (both generator and detector flywheel spinning) as described by Wallace was not possible to realize. The oscillation of the detector is harmonic but damped, so it is impossible to measure about a time scale of more than 10 minutes without reinitiating it. The measurement of the oscillation period and amplitude was realized with a laser diode. A mirror, which was fixed at the detector, reflected the light beam to a linear photo diode. This set-up enabled a highly precise measurement of the detector oscillation. A reference measurement of an oscillation without any action of the generator is shown in **Fig. 10**. To determine the tolerance of the amplitude and the cycle duration, several reference measurements were made.
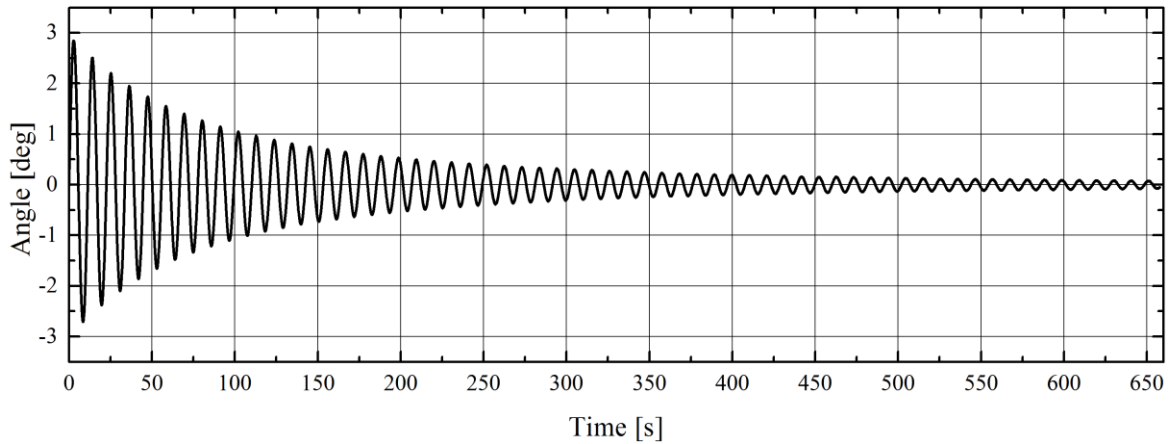
Figure 10   Reference measurement of the oscillating detector over a period of 10 minutes.

In consequence of the influence of the bearing friction and the flow resistivity, the period time and the amplitude are non-lineal and it is difficult to compare one section of the oscillation with another one of the same oscillation. **Fig. 11** shows the modifications of the amplitude and the periodic time over the total number of periods in measurement duration of 10 minutes.

In the beginning of the oscillation, the amplitude starts with an angle of nearly three degrees (similar to Wallace's measurement) but it is damped because of friction. In the end the percentage of the bearing friction rises with the consequence of an increased period duration. These characteristics are caused by the fact that the used pendulum is not ideal. The consideration of its geometrical dimensions makes it necessary to use the equation for the aerodynamic resistance to explain the non-linearity. With
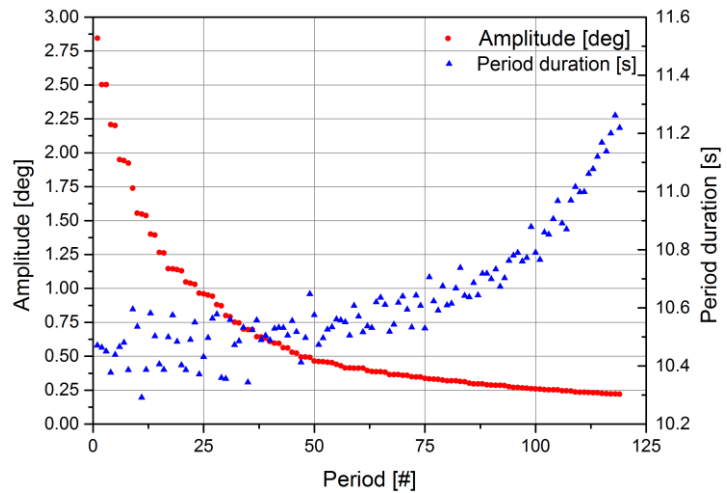

Figure 11   Correlation of the amplitude and the period duration over a complete oscillation of the detector.

$$F_W = \frac{\rho c_W A}{2} v^2 \qquad (4)$$

it is apparent that the aerodynamic resistance is directly dependent to the square velocity of the pendulum by passing the position of rest. This explains the strong damping while starting at higher amplitudes. It is clear that it is impossible to take a statement of the influence of a creating force field within one oscillation. To measure a possible force field it is necessary to take comparison between measurements with different set-up conditions.

Starting the experiment by using the set-up conditions of Wallace, it seemed that there was indeed an effect caused by the rotating flywheel. **Fig. 12** shows one of the first measurement results with the oscillating detector. While the detector assembly has been arranged in rest position the flywheel started to rotate. During the time of acceleration up to a velocity of approximately 29,000 rpm, the detector started to oscillate, deflected to a short maximum of nearly 7 degrees and moved back to an area next to the rest position. After turning off the compressed air, the detector reacted at discrete values of rotation speeds. This fact suggested the assumption that micro vibrations of the rotating generator flywheel were transferred over the structural components to the detector and induced uncontrollable effects.
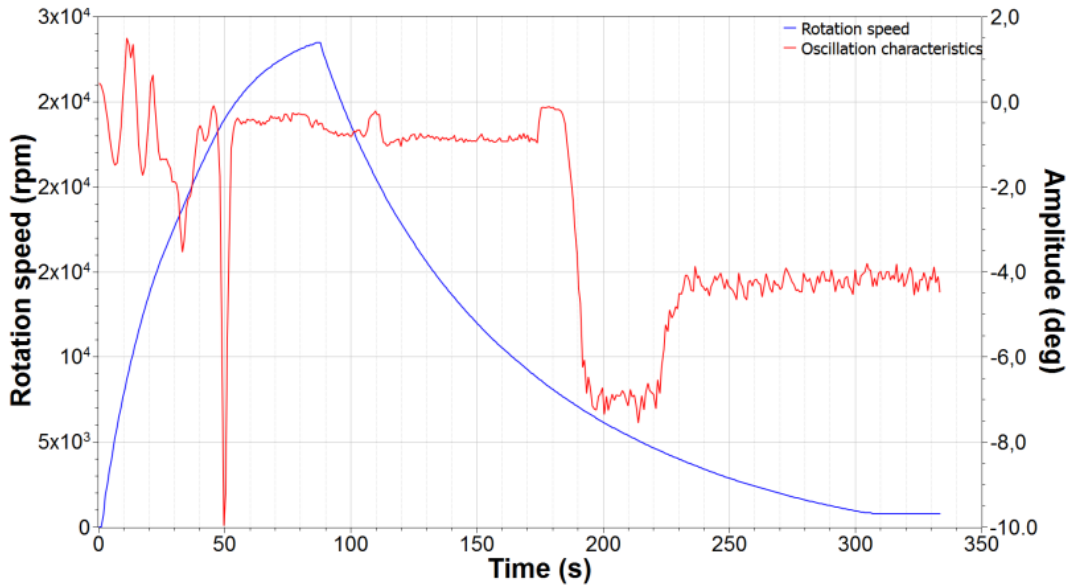
Figure 12 Reaction of the non-oscillating detector to the rotating flywheel in Wallace's original setup configuration (observed anomaly).

To eliminate this possibility, the complete detector assembly was mounted on a separate stand and installed independent from the structure on a separate workbench. After this modification the effects did not occurred again and the measurement results were comparable to the reference measurements. The modified configuration is shown in **Fig. 13**. Additionally a closed case was installed to protect the sensitive detector from the airflow of the compressed air.
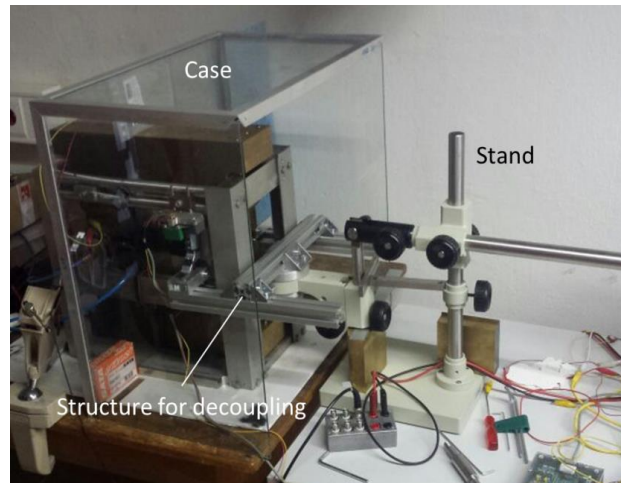
To understand the reason for the extreme sensitivity for vibrations of the detector with this high mass, it is necessary to recall the equations for a real pendulum and the correlation of its center of mass and the suspension point. By considering the equation for a physically pendulum again and additionally using the theorem of Steiner

Figure 13 Modified configuration of the redesigned setup.

$$T = 2\pi\sqrt{\frac{J}{mgr}}, \text{ with } J = J_0 + mr^2 \tag{5}$$

the equation for the angular velocity is

$$\omega^2 = \frac{mgr}{J_0 + mr^2}. \tag{6}$$

Converting this equation to the distance between the center of mass and the suspension point "r" we will receive two possible solutions for r with the same periodic time. So this kind of pendulum is a special type called Kater's

American Institute of Aeronautics and Astronautics

pendulum. The solutions for "r" in this case are: r_1=30.25m and r_2=0.64mm (6.4x10^{-4}m). This is the distance that was used in Wallace's original and our redesigned experimental set-up and it can explain the extremely high sensibility of a mass of more than 10 kilograms.

Fig. 14 shows measurements for our vibration-free setup with the detector oscillating and the generator at rest and under rotation (in CW and CCW direction). We further improved the setup by implementing plexi-glass shielding of the detector assembly in order to reduce any air flow. The measurements were made while running down the generator flywheel after it reached its final speed and the results were standardized (in time) and superposed starting with the first local maximum at an angle of lower than three degrees. We can see that the phase displacement between the two graphs (CW and CCW) and the reference graph is too small (less than 2.5 seconds) to see a significant effect. Also a clear difference between the amplitudes of the single measurements is not visible. From our measurements we cannot see any difference between CW and CCW rotation to <0.1 degrees which is 4 times lower than Wallace's claim of 0.4 degrees. We can therefore conclude that Wallace's anomalous signal must have been due to vibrations that can be completely removed by proper isolation as described above.
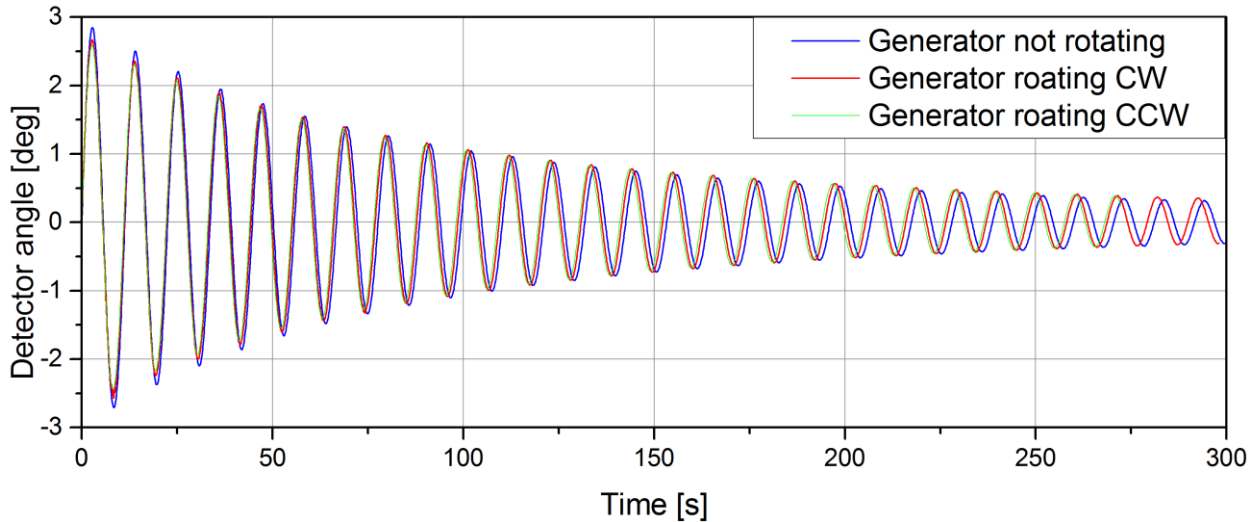

Figure 14   Comparison of three representative oscillation measurements with different set-up conditions. The blue graph is a reference measurement (without energized flywheel), the red graph is a measurement with clockwise energized flywheel and the green graph for the counterclockwise direction.

V.   Conclusion

Here we explored for the first time experimentally the claims of Wallace that high-speed rotation of nuclear spin-polarizable mass generates an anomalous large frame dragging/a measureable gravitational-like field. Based on three patent descriptions, we redesigned and manufactured his experimental setup to verify his claims. We optimized the whole experimental setup in order to ensure a safe operation at the required high rotation speeds and allow ease of operation. After building the setup, we implemented three different measurement procedures in addition to Wallace's solution by observing the field with a pendulum. While the measurements with the additional systems - the Hall sensors, the accelerometers and the gyroscope - did not show any significant effect, it was possible to detect a reaction by using the oscillating detector as described by Wallace (however, our detector was not spinning). By decoupling the oscillator from the rest of the experimental set-up's vibration with an additional support structure, the effect disappeared. A further modification to the set-up was also done by installing an enclosure around the generator to protect the detector from airflow. This resulted in an increase of the measurement's accuracy with the oscillating detector and it could be shown that vibrations of the generator flywheel and the primary and secondary airflow of its energizing compressed air caused the generated effect.

In conclusion, we have shown that no gravitational-like field was generated with a better accuracy compared to the original claim and that vibrations transferred from the generator flywheel caused the Wallace effect.

References

[1]Wallace, H. W., *Method and Apparatus for generating a secondary gravitational force field*, US-Patent 3,626,605, 1971

[2]Wallace, H. W.; *Method and Apparatus for generating a dynamic force field*, US-Patent 3,626,606, 1971

[3]Wallace, H. W., *Heat Pump,* US-Patent 3,823,570, 1974

[4]Barnett, S. J., *Magnetization by Rotation*, Phys. Rev., Vol. 6*,* 1915, pp. 239-270

[5]Lense, J., Thirring, H., *Über den Einfluss der Eigenrotation der Zentralkörper auf die Bewegung der Planeten und Monde nach der Einsteinschen Gravitationstheorie*, Physikalische Zeitschrift, Vol. 19, 1918, pp. 156–163

[6]Tajmar, M., Plesescu, F., and Seifert, B., *Anomalous Fiber Optic Gyroscope Signals Observed above Spinning Rings at Low Temperature*, J. Phys.: Conf. Series, Vol. 150, 2009, pp. 032101

[7]Grugel, R.N., Volz, M.P., Mazuruk, K., *An experimental investigation to determine interaction between rotating bodies,* Final Report, MSFC/NASA, NASA TM-2003-2 1 2286, 2003